STRUCTURAL CONTROL AND HEALTH MONITORING
Struct. Control Health Monit. 2006; **13**:536–552
Published online 19 December 2005 in Wiley InterScience (www.interscience.wiley.com). DOI: 10.1002/stc.128

Active control of structures using time delayed positive feedback proportional control designs

Firdaus E. Udwadia[1,2,*,†,‡] and Phailaung Phohomsiri[1,§]

[1] *Aerospace and Mechanical Engineering, University of Southern California, Los Angeles, CA 90089-1453, U.S.A.*
[2] *Civil Engineering, Mathematics and Information and Operations Management, University of Southern California, Los Angeles, CA 90089-1453, U.S.A.*

SUMMARY

This paper explores a new methodology for the active control of structures through the use of time delayed, positive feedback proportional control. The idea is to utilize *intentional* time delays, which may not necessarily be small when compared with the natural periods of vibration of a structure. Such time delayed systems are infinite dimensional. Analytical and computational results related to both system and non-system poles are herein provided for the first time. Results related to the stability of the presented control methodology are given. The efficacy of the control design is illustrated by applying it to a structure modelled as a single-degree-of-freedom system subjected to strong earthquake ground shaking. It is shown that while displaying good stability characteristics, the performance of such time delayed positive feedback proportional control can be even superior—in terms of both, reduced structural response, and reduced control effort—to standard proportional negative feedback control designs with no time delay. Copyright © 2005 John Wiley & Sons, Ltd.

KEY WORDS: time delay; structural control; structural dynamics; positive feedback; proportional control; system stability; system performance; earthquake hazard mitigation; non-system poles; system poles

1. INTRODUCTION

Time delays arise unavoidably in the active control of engineering structures due to delays in sensing structural vibrations, filtering data, calculating control forces, and applying the computed control forces. The problem of time delays in the active control of structural systems has been investigated by many scientists and engineers [1–10]. However, most of them have developed techniques based on the premise that such time delays are injurious to the control system, that they are, or should be kept, small compared to the fundamental period of vibration

*Correspondence to: F. E. Udwadia, Aerospace and Mechanical Engineering, Civil Engineering, Mathematics and Information and Operations Management, 430k Olin Hall, University of Southern California, Los Angeles, CA 90089-1453, U.S.A.
† E-mail: fudwadia@usc.edu, fudwadia@adelphia.net
‡ Professor.
§ Postdoctoral Research Associate.

Received 30 May 2005
Revised 6 September 2005

of the system, and that they need to be eliminated and/or compensated for [7, 8]. Yet, often times in large complex structures, time delays that are a considerable portion of a natural frequency of the structure can arise [11, 12]. This paper continues a recent and novel line of thinking that time delays, which in any case arise naturally in closed loop control systems, when purposively injected in a structural control system may be used to good benefit in the design of active control of structures.

Initial work done in the area of time delayed structural control suggested that small time delays—small, compared to the fundamental natural period of a structural system—in the feedback control loop could have a beneficial effect on non-collocated structural control designs [13–18]. Udwadia *et al*. [19] investigate the use of velocity feedback control while intentionally introducing large time delays in the control loop. They use time delays in the vicinity of the natural period of the system. They analytically study the stability and performance of their control design and illustrate its efficacy using structures modelled as single and multi-degree-of-freedom systems. They then expand their control design [20] to include time delays in the vicinity of half the natural period of the system and use instead positive velocity feedback. They show that performance and stability of the time delayed velocity feedback control are satisfactory, and that positive feedback leads to improved performance with reduced control effort, when compared to time delayed negative velocity feedback.

In this paper, we present proportional control with positive feedback—what we call, for short, *p*ositive *p*roportional *f*eedback control, or PPF—that uses intentional time delays that may not necessarily be small compared with the natural periods of the structural system. That such control is feasible is not entirely intuitive, for we know that when there is no time delay, positive feedback proportional control can become unstable (see details in Section 4). What is far less intuitive is that such control can be even more efficacious than standard negative feedback proportional control. And it is perhaps here that the novelty of the results presented herein lie. We investigate stability and performance issues related to time delayed PPF control and present several new results related to the behaviour of the closed loop control system. Compared with standard negative proportional feedback control methodologies with no time delay, we show that the new control methodology is very efficient both in the control effort used and in the reduction of the structural response, while maintaining good stability characteristics. In a different context, Olgac and Holm-Hansen [21] used time delayed proportional feedback for designing vibration absorbers, which they call delayed resonators. Their approach [21, 22] differs from that presented here because: (1) they emphasize the use of negative feedback, (2) they select control gains and time delays to obtain their dominant resonator poles on the imaginary axis, (3) they ignore interactions between the so-called system poles and the non-systems poles, (4) and they consider only sinusoidal excitations. In this paper we use, instead, positive proportional feedback. We show that a variety of time delays and control gains are effective, and lead to robust control, in general excitation environments such as during strong earthquake ground shaking.

The structure of this paper is as follows. We study the behaviour of the so-called 'system poles' in Section 2. In Section 3 we present the behaviour of the so-called 'non-system poles' caused by the infinite dimensionality of the time delayed system. In Section 4 stability analysis of time delayed positive proportional feedback control is provided. We then apply this control methodology to an SDOF system in Section 5 and demonstrate its superiority in terms of performance when compared with standard negative proportional feedback control. Lastly, we provide our conclusions in Section 6.

2. BEHAVIOUR OF SYSTEM POLES

Let us start with considering a single-degree-of-freedom (SDOF) system subjected to excitation with time delayed proportional feedback

$$\ddot{x} + 2\omega_n\zeta_n\dot{x} + \omega_n^2 x = g_p x(t - T_d) + f(t) \tag{1}$$

where ω_n and $0 < \zeta_n \ll 1$ are the natural frequency and the damping ratio of the uncontrolled system, respectively. The first term on the right-hand side of Equation (1) represents *positive* proportional feedback that is delayed by a time $T_d > 0$ with a gain $g_p > 0$, and the second term, $f(t)$, represents the external excitation.

Taking the Laplace transform of Equation (1) to obtain the characteristic equation of the system, we have (with $f(t) = 0$),

$$s^2 + 2\omega_n\zeta_n s + \omega_n^2 - g_p \exp(-sT_d) = 0 \tag{2}$$

which can be written in normalized form as

$$\tilde{s}^2 + 2\zeta_n\tilde{s} + 1 - \gamma_p \exp(-2\pi\tau\tilde{s}) = 0 \tag{3}$$

where, $\tilde{s} = s/\omega_n$, $\tau = T_d/T_n = \omega_n T_d/2\pi$, and $\gamma_p = g_p/\omega_n^2 > 0$ (positive feedback).

When $g_p = 0$, the complex conjugate roots of Equation (2), the so-called 'system poles', are given by

$$s_{1,\bar{1}} = -\omega_n\zeta_n \pm i\omega_n\sqrt{1 - \zeta_n^2} \tag{4}$$

which can also be expressed in normalized form as

$$\tilde{s}_{1,\bar{1}}(\omega_n, \zeta_n) = -\zeta_n \pm i\sqrt{1 - \zeta_n^2} \tag{5}$$

When we increase the gain $g_p > 0$, the locations of these system poles change, because they now become functions of the time delay T_d and the gain g_p. For convenience they can again be expressed, similar to Equation (4), as

$$s_{1,\bar{1}}(T_d, g_v; \omega_n, \zeta_n) = -\tilde{\omega}_n\tilde{\zeta}_n \pm i\tilde{\omega}_n\sqrt{1 - \tilde{\zeta}_n^2} \tag{6}$$

where $\tilde{\omega}_n(T_d, g_v)$ and $\tilde{\zeta}_n(T_d, g_v)$ are the equivalent natural frequency of vibration and the equivalent damping factor, respectively. Similarly, we write Equation (6) in the normalized form as

$$\tilde{s}_{1,\bar{1}}(\tau, \gamma_v; \zeta_n) = -\tilde{\zeta}_n r \pm ir\sqrt{1 - \tilde{\zeta}_n^2} \tag{7}$$

where the normalized equivalent natural frequency $r = \tilde{\omega}_n/\omega_n$. The equivalent natural frequency of vibration and the equivalent damping factor given in Equation (6) are obtained from the relations

$$\tilde{\zeta}_n(T_d, g_v) = \frac{\delta}{\sqrt{1 + \delta^2}} \tag{8}$$

and

$$\tilde{\omega}_n(T_d, g_v) = \frac{\mathrm{Im}[s_1(T_d, g_v)]}{\sqrt{1 - \tilde{\zeta}_n^2}} \tag{9}$$

where

$$\delta = -\frac{\mathrm{Re}[s_1(T_d, g_v)]}{\mathrm{Im}[s_1(T_d, g_v)]} \tag{10}$$

Because the characteristic equation of the time delayed system is non-linear, it is difficult to find its roots analytically; however, the roots can be obtained computationally. We start with finding the locations of the system poles when $\gamma_p = 0$, and then use these locations as initial guesses for finding the system poles (using a root finding algorithm) for a value of γ_p that is 'slightly' increased from zero. We then use the pole locations so found again as initial guesses for finding the system poles when the gain is increased by yet another small increment, and so on. The poles so obtained will be called the 'system' poles.

Figure 1 shows the root loci of the system poles for different time delays as the gain γ_p increases from 0 to 1.4 units. Since the poles come in conjugate pairs, we show the root loci only in the upper half complex plane. All the root loci start from $(-\zeta_n, \sqrt{1-\zeta_n^2})$ when $\gamma_p = 0$. Each root locus is for a different value of the normalized time delay τ. For example, we see from the root locus for $\tau = 0.2$, that as the gain increases from $\gamma_p = 0$, the root locus moves to the left. As we keep increasing the gain, γ_p, the root locus continues moving leftward until $\gamma_p \approx 0.7$. As the gain γ_p increases further, the root locus appears to bend over towards the right half complex plane. As seen from the figure, the root loci seem to swing around clockwise as the normalized time delay τ increases.

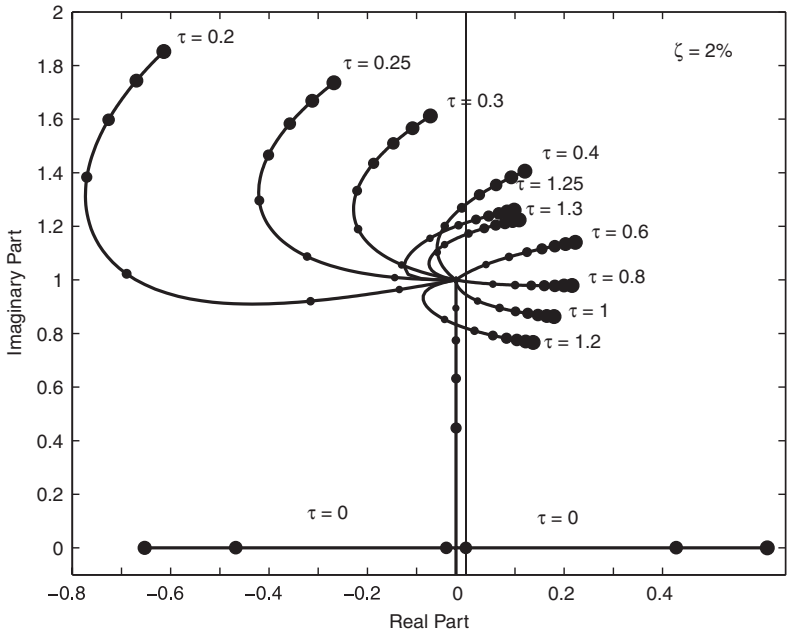

Figure 1. Root loci of the system poles for positive proportional feedback control with different dimensionless time delays, τ. The successively larger solid dots along each curve show the location of the poles as the dimensionless gain γ_p increases from 0 to 1.4 units in increments of 0.2. The damping factor of the uncontrolled system is $\zeta_n = 2\%$.

In the absence of any time delay, as the gain γ_p increases from zero, the frequency of vibration of the controlled system drops. The real part of the root locus for $\tau = 0$ in Figure 1 remains unchanged, while the imaginary part decreases for $0 < \gamma_p < 1 - \zeta_n^2$ and reaches zero when $\gamma_p = 1 - \zeta_n^2$. A further increase in the gain causes the root locus to split into two branches, the poles along each branch moving in opposite directions. The rightward moving pole reaches the imaginary axis when $\gamma_p = 1$, beyond which the system pole crosses into the right half complex plane. Thus proportional positive feedback control with no time delay is stable for $\gamma_p < 1$.

Next, we provide some analytical results dealing with the behaviour of the system poles. Starting with differentiating Equation (3), we have

$$\frac{d\tilde{s}}{d\gamma_p} = \frac{1}{2}\left[\frac{\exp(-2\pi\tau\tilde{s})}{(\tilde{s}+\zeta_n) + \pi\tau\gamma_p \exp(-2\pi\tau\tilde{s})}\right] \tag{11}$$

When $\gamma_p \to 0$, we have

$$\lim_{\gamma_v \to 0} \frac{d\tilde{s}}{d\gamma_p} = \frac{1}{2}\frac{\exp(-2\pi\tau\tilde{s})}{\tilde{s}+\zeta_n} \tag{12}$$

Since $\tilde{s}_{1,\bar{1}}(\tau, \gamma_p \to 0; \zeta_n) \approx -\zeta_n + i\sqrt{1-\zeta_n^2}$ (we consider only the upper half plane), Equation (12) yields

$$\lim_{\gamma_p \to 0} \frac{d\tilde{s}}{d\gamma_p} = \lim_{\gamma_p \to 0}\left[\frac{d\,\mathrm{Re}(\tilde{s})}{d\gamma_p} + i\frac{d\,\mathrm{Im}(\tilde{s})}{d\gamma_p}\right] = \frac{1}{2}\frac{\exp(2\pi\tau\zeta_n)\exp(-2\pi\tau i\sqrt{1-\zeta_n^2})}{-\zeta_n + i\sqrt{1-\zeta_n^2} + \zeta_n}$$

$$\approx -\frac{1}{2}\exp(2\pi\tau\zeta_n)[\sin(2\pi\tau + i\cos(2\pi\tau)] \quad \text{for } \zeta_n \ll 1 \tag{13}$$

Equation (13) shows that the slope of each root locus for different time delays is approximately $\cot(2\pi\tau)$ as $\gamma_p \to 0$. For example, as seen in Figure 1, the system pole moves leftwards with the slopes of about 18.6°, 0°, -18.8°, and -78.9° for $\tau = 0.2, 0.25, 0.3$, and 0.4, respectively, for $\gamma_p \approx 0$.

In Figure 2, we demonstrate the equivalent damping factor, $\tilde{\zeta}_n$, of the positive proportional feedback system as a function of the gain γ_p for different time delays, $\tau = 0.2, 0.25, 0.3, 0.4, \ldots, 1.2, 1.25, 1.3$. The damping factor of the uncontrolled system that we use here is $\zeta_n = 2\%$. The figure shows that the equivalent damping factors for $\tau = 0.2, 0.25$, and 0.3 are high, where the highest values are approximately 0.57, 0.31, and 0.17, respectively. Thus, for time delayed proportional feedback control design purposes, one might want to take advantage of using dimensionless time delays, τ, in the range [0.2–0.3] with corresponding gains where the equivalent damping factors are highest.

Figure 3 shows the normalized equivalent natural frequency as a function of the gain γ_p for different time delays, τ. Each curve corresponds to a different value of the time delay. The curves show that as the gain is increased, the normalized equivalent natural frequency, r, increases for values of $\tau = 0.2, 0.25, 0.3, 0.4, 0.6, 1.25$, and 1.3.

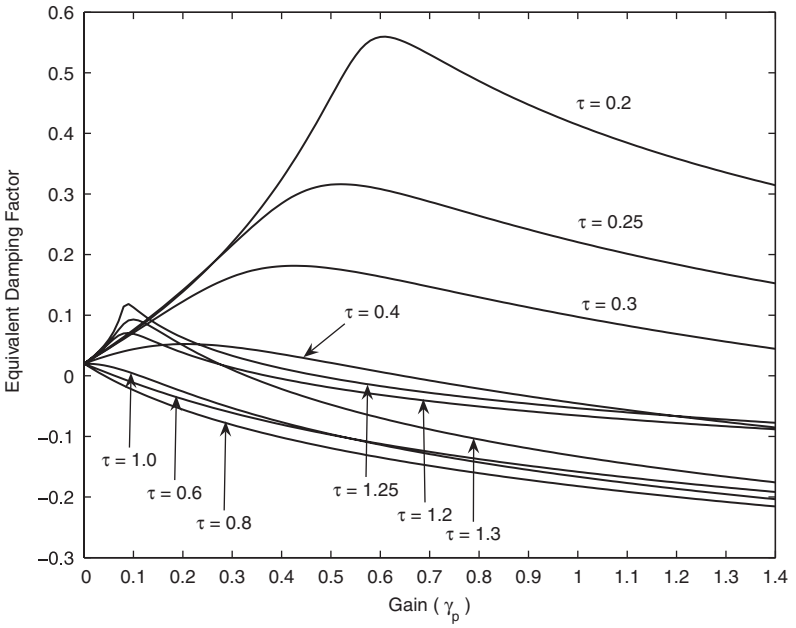

Figure 2. Equivalent damping factor $\tilde{\zeta}_n$ as a function of the gain γ_p for system poles for positive proportional feedback control with different time delays τ.

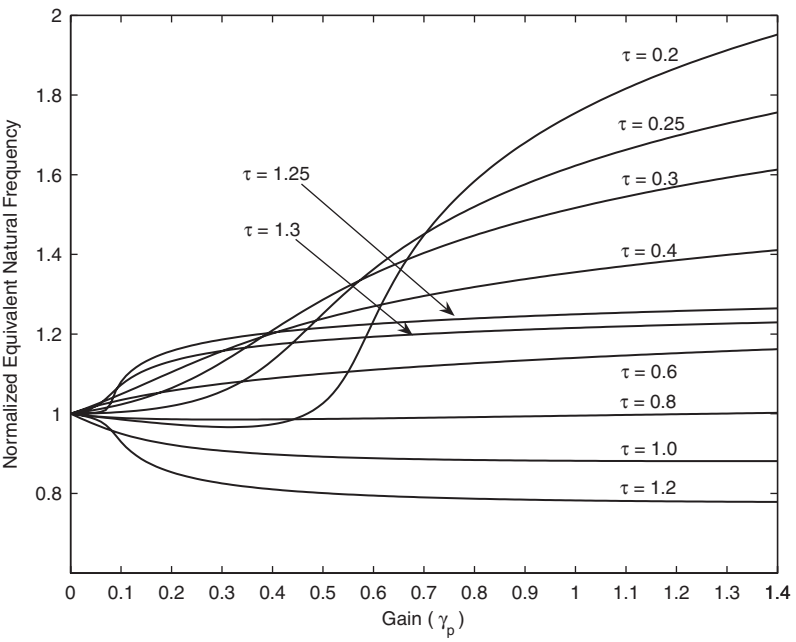

Figure 3. Normalized equivalent natural frequency, $r = \tilde{\omega}_n/\omega_n$, as a function of the gain γ_p for positive proportional feedback control system with different time delays τ.

3. BEHAVIOUR OF NON-SYSTEM POLES

When the time delay becomes large, compared to the natural frequency of vibration of the system, one needs to consider the effect of the non-system poles, as suggested by Udwadia *et al.* [19]. These are the poles that arise at the far left-hand end of the complex plane $\tilde{s}$-plane when the control gain $\gamma_p = 0^+$, and they stream in rightwards into the complex plane as the control gain γ_p increases. We shall call these poles the 'non-system' poles. There are infinitely many of them, thus making the controlled system infinite dimensional. In this section, we shall study the behaviour of these non-system poles and show that they, in fact, can control the stability of the time delayed control design.

As shown in Figure 4, the non-system poles start at the extreme left end of the complex plane; each pole makes its way rightwards as the gain is increased. Though there are an infinite number of poles we only show a set of 5 poles, for two different values of the time delay: $\tau = 0.2$ and 0.3. Similar behaviour of the non-system poles is observed for values of τ in the range [0.2, 0.3]. We observe that the rate of vertical change of the root loci is, comparatively speaking, smaller than the rate of horizontal change. Also, the spacing between any two of the upper four root loci shown seems to be approximately a constant. We shall subsequently show the analytical reasons for this behaviour.

The lowest non-system pole (see Figure 4) in the upper-half complex plane travels rightwards along the real axis as the gain is increased, and is the first to reach the imaginary axis among all the poles (system and non-system). It is this non-system pole that controls the stability of the time delayed control system in the range of time delays shown in Figure 4. In fact, for $0 \leqslant \tau \leqslant 0.36$ (see Figure 5) the pole that first crosses the imaginary axis is always the one that moves along the real axis in the complex plane; it crosses over into the right half complex plane when $\gamma_p = 1$.

We next obtain some analytical results to get more insights into the behaviour of these non-system poles, and hence explain some of the above-mentioned observations.

Equation (3) can be rewritten as $\exp(-2\pi\tau\tilde{s}) = (\tilde{s}^2 + 2\zeta_n\tilde{s} + 1)/\gamma_p$. Using this in Equation (11), we have

$$\frac{\mathrm{d}\tilde{s}}{\mathrm{d}\gamma_p} = \frac{1}{2\gamma_p}\frac{1}{\pi\tau + \dfrac{\tilde{s} + \zeta_n}{\tilde{s}^2 + 2\zeta_n\tilde{s} + 1}} \tag{14}$$

Let us define

$$\tilde{s} = R\exp\{\mathrm{i}(\pi - \varphi)\} = -R\exp(-\mathrm{i}\varphi) \tag{15}$$

where R is a positive, real number, and φ is the angle measured from the negative real axis in the clockwise direction. For $R >> 1$, we then obtain, using Equation (15)

$$\begin{aligned}\frac{\mathrm{d}\tilde{s}}{\mathrm{d}\gamma_p} &\approx \frac{1}{2\gamma_p}\frac{1}{\pi\tau + \dfrac{1}{\tilde{s}}} = \frac{1}{2\gamma_p}\frac{1}{\pi\tau - \dfrac{\exp(\mathrm{i}\varphi)}{R}} \\ &= \frac{1}{2\gamma_p}\frac{1}{\pi\tau - \dfrac{\cos\varphi + \mathrm{i}\sin\varphi}{R}} \approx \frac{1}{2\gamma_p}.\frac{R\pi\tau - \cos\varphi + \mathrm{i}\sin\varphi}{R(\pi\tau)^2 - 2\pi\tau\cos\varphi}\end{aligned} \tag{16}$$

For $\pi\tau R >> 1$, this yields

$$\frac{\mathrm{d}\tilde{s}}{\mathrm{d}\gamma_p} \approx \frac{1}{2\pi\tau\gamma_p} + \mathrm{i}\,\frac{\sin\varphi}{2\pi^2\tau^2 R\gamma_p} \tag{17}$$

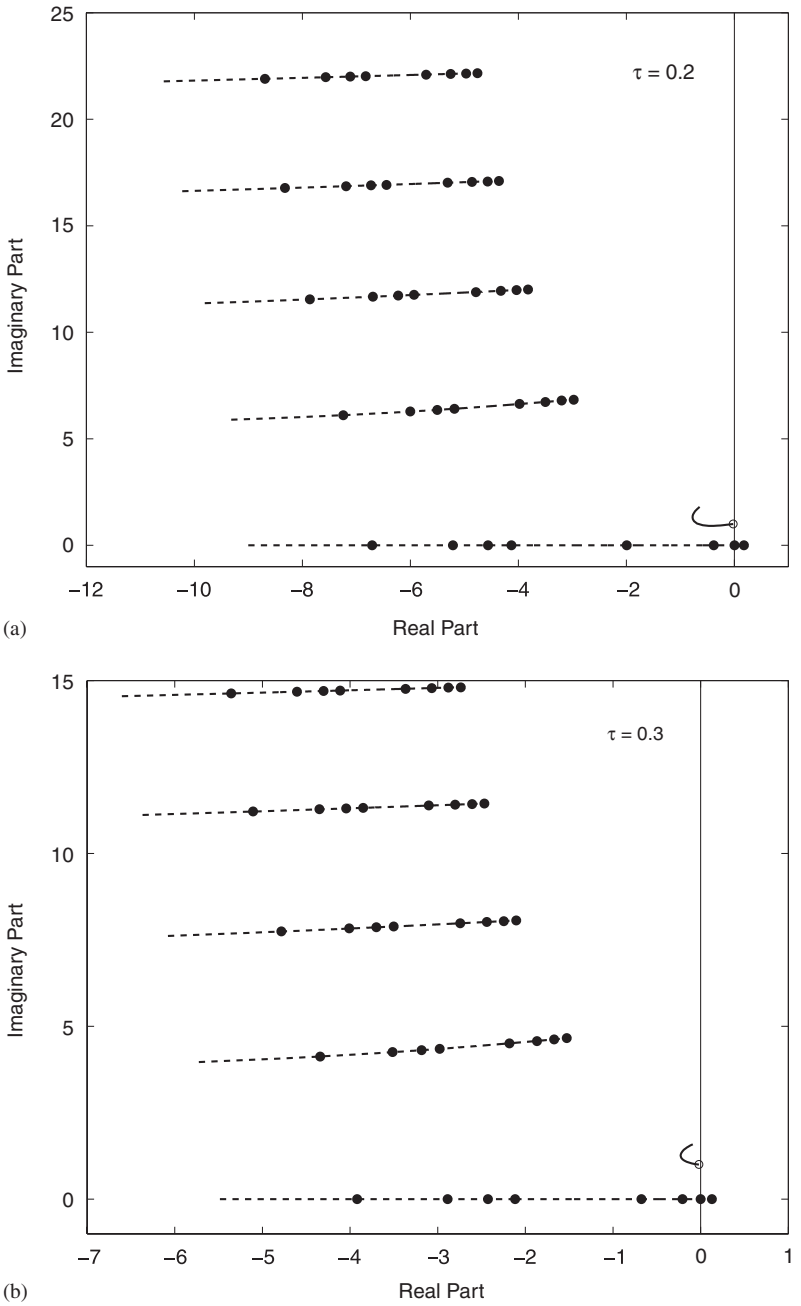

Figure 4. The root loci of both system and non-system poles for proportional feedback system for dimensionless time delays: (a) $\tau = 0.2$; and (b) $\tau = 0.3$ for $\zeta_n = 2\%$. Solid dots along each root locus represent the locations of the non-system poles at gains $\gamma_p = 0.01, 0.04, 0.07, 0.1, 0.4, 0.7, 1.0$, and 1.3; the left-most point along each root locus is the location of the pole at $\gamma_p = 0.001$. The solid line shows the root locus of the system pole starting with the open circle where $\gamma_p = 0$. Only the upper half complex plane is shown.

Equation (17) says that the rate of change of the real part of the system poles with respect to gain is (approximately) inversely proportional to the product of $\tau\gamma_p$, while the rate of change of the imaginary part, is inversely proportional to $\tau^2 R\gamma_p$, which of course is much smaller than that of the real part for $R >> 1$. This means that the non-system poles move with greater speed rightwards than upwards in the complex plane, as shown in Figure 4.

We next provide analytical estimates for the locations of the root loci of the non-system poles when crossing the imaginary axis and then determine the gains at which these non-system poles cross the imaginary axis.

Let us first substitute Equation (15) in Equation (3) to get

$$R^2\left[1 - \frac{2\zeta_n \exp(\mathrm{i}\varphi)}{R} + \frac{\exp(\mathrm{i}2\varphi)}{R^2}\right] = \gamma_p \exp(2\mathrm{i}\varphi)\exp(2\pi\tau R\cos\varphi)\exp(-\mathrm{i}2\pi\tau R\sin\varphi) \tag{18}$$

Taking logarithms on both sides of Equation (18), and expanding the logarithm, we obtain

$$\left[\ln R^2 - \ln\gamma_p - 2\pi\tau R\cos\varphi - \left(\frac{2\zeta_n\cos\varphi}{R} - \frac{\cos 2\varphi}{R^2} + \cdots\right)\right] + \mathrm{i}\left[-2\varphi + 2\pi\tau R\sin\varphi - 2n\pi - \left(\frac{2\zeta_n\sin\varphi}{R} - \frac{\sin 2\varphi}{R^2} + \cdots\right)\right] = 0, \quad n = 0, \pm 1, \pm 2, \ldots \tag{19}$$

When the non-system poles cross the imaginary axis ($\varphi = \pi/2$), the imaginary part of Equation (19) yields

$$R \approx \frac{1}{2\tau}[2n+1], \quad n = 1, 2, 3, \ldots \text{ for } R >> 1 \tag{20}$$

while the real part of the equation gives

$$\gamma_p \approx R^2 \exp\left(-\frac{1}{R^2}\right) \quad \text{for } R >> 1 \tag{21}$$

Using Equation (20) in Equation (21), we have

$$\gamma_p \approx \frac{1}{4\tau^2}(2n+1)^2 \exp\left[-\frac{4\tau^2}{(2n+1)^2}\right], \quad n = 0, 1, 2 \ldots \tag{22}$$

From relation (20), the spacing between each root locus is about $1/\tau$, which is consistent with the computational results seen in Figure 4. Relation (20) estimates the locations of the root loci of the non-system poles when they cross the imaginary axis. For example, for the non-system pole described by $n = 2$, using relation (20) we get $R \approx 12.5$ for $\tau = 0.2$; this means that the pole crosses the imaginary axis at about a vertical distance of 12.5 from the real axis. Direct numerical simulation yields a value of 12.506, in close agreement with our analytical result.

Relation (22) estimates the value of the gain at which the non-system poles cross the imaginary axis. For $n = 2$, the gain, γ_p given by this equation is 155.25 for $\tau = 0.2$. Direct numerical simulation gives a value of 155.31 for the gain γ_p when this pole crosses the imaginary axis, again in close agreement with relation (22). Similar results are found for the non-system poles described by other values of $n > 2$, showing that relations (20) and (22) provide good approximations for both the frequencies at which the poles cross the imaginary axis and the values of the gains at which this happens.

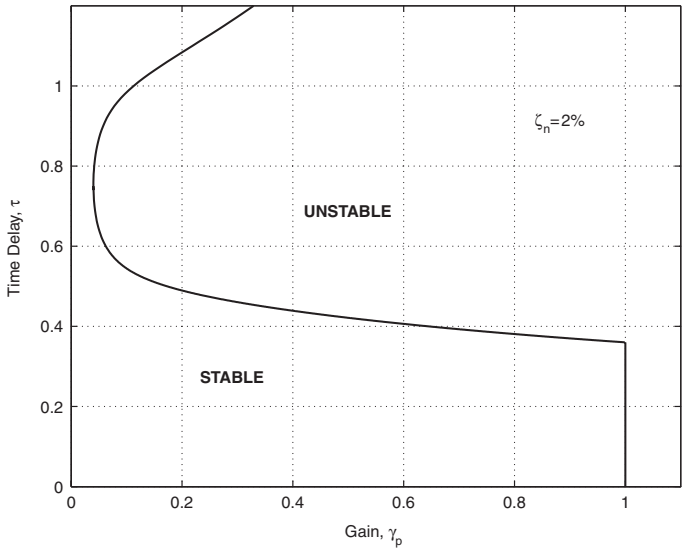

Figure 5. Plot of positive feedback gain versus time delay showing stability zones for time delayed proportional feedback control with $\zeta_n = 2\%$ over the range $0 \leqslant \tau \leqslant 1.2$.

4. STABILITY OF TIME DELAYED POSITIVE FEEDBACK PROPORTIONAL CONTROL SYSTEM

In this section, we consider issues of stability related to the time delayed positive feedback proportional control system. We investigate the minimum gain at which the first pole (system or non-system) crosses over into the right half complex plane. Due to limitations of space we do not derive the analytical stability results here, but provide them, by way of illustration, in Figure 5 for a system with $\zeta_n = 2\%$.

From Figure 4 we see that for τ in the range [0.2–0.3], as the gain is increased, it is the non-system pole, which comes along the real axis as we gradually increase the gain, that first crosses the imaginary axis at the co-ordinate (0,0), thereby dictating the stability of the system. To find the gain at which a pole that moves along the real axis crosses over into the right half complex plane, we substitute $\tilde{s} = 0$ in Equation (3). Hence, we obtain the gain $\gamma_p = 1$, which is the maximum gain for which the structural system remains stable (see Figure 5).

In fact, the stability of the controlled system can be dictated by either the system or the non-system poles, depending on the value of the time delay τ. For values of the time delay $0 \leqslant \tau < 0.159$, the root locus picture for the system poles is quite complex because they interact with the non-system pole that comes along the real axis. For this range of time delays, it is the system pole, which moves along the real axis as the gain is steadily increased, that first crosses over into the right half complex plane; the maximum gain for stability is then unity. For time delays $0.159 \leqslant \tau \leqslant 0.36$, it is now the non-system pole, which again moves along the real axis as the gain is steadily increased, that dictates the stability of the system; as before, the maximum gain for stability remains unity in this range of time delays as well (see Figure 5). However, for larger

time delays $\tau > 0.36$, the stability of the time delayed system can be dictated by the system poles. Furthermore, it can be shown that for values of the gain $\gamma_p < 2\zeta_n\sqrt{1-\zeta_n^2}$ the time delayed system is stable for all values of the time delay τ.

5. APPLICATION TO STRUCTURAL CONTROL

In this section, we apply time delayed positive proportional feedback (PPF) control to a single-degree-of-freedom (SDOF) structural system subjected to a base acceleration, which simulates strong earthquake ground shaking. To establish the efficacy of the control methodology, we compare it with standard (negative) proportional feedback (NPF) control with no time delay.

Consider the structural system modelled by an SDOF system which has a damping factor $\zeta_n = 2\%$ and a natural period $T_n = 0.804$ s. It is subjected to the synthetically generated ground acceleration shown in Figure 6. We consider a positive proportional feedback control design with a time delay $\tau = 0.25$, and a control gain $\gamma_p = 0.5$. This design gain is chosen to give a high value of the equivalent damping factor (see Figure 2). Since its value is well below the gain at which the time delayed system becomes unstable, i.e. below $\gamma_p = 1$ (see Figures 4 and 5), the chosen time delayed control design is guaranteed to be stable. For comparison, the same control gain is used for both time delayed positive proportional feedback (PPF), and for standard (negative) proportional feedback (NPF) with no time delay. We also draw comparisons between time delayed PPF control, and NPF control with a much larger gain of $\gamma_p = 3$.

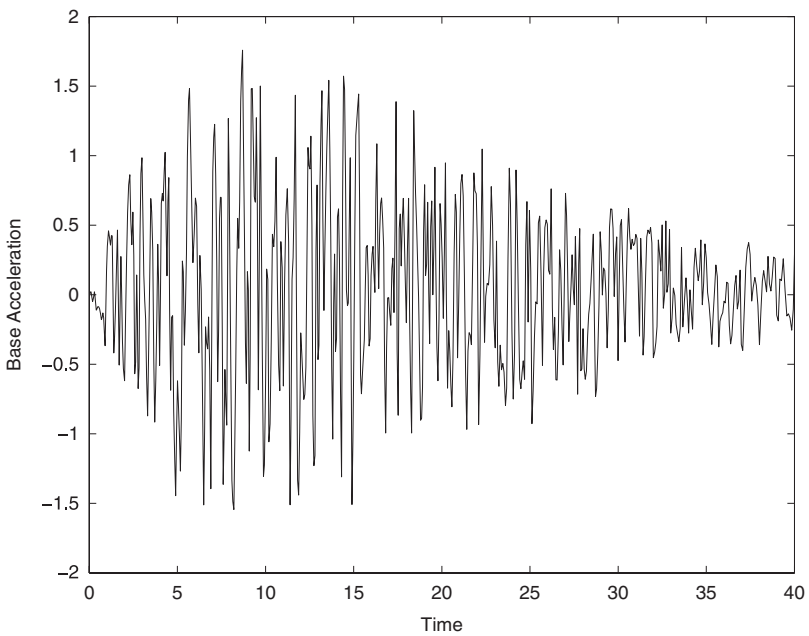

Figure 6. Base acceleration as a function of time.

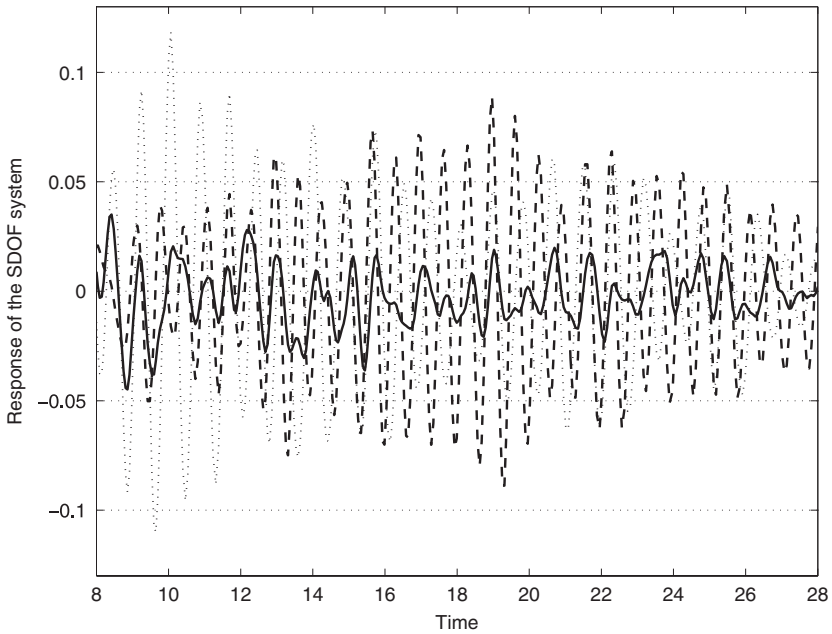

Figure 7. Comparison of the large amplitude response of the SDOF system: using no control (dotted line); using PPF control with $\tau = 0.25$ and $\gamma_p = 0.5$ (solid line); and using NPF control with no time delay and $\gamma_p = 0.5$ (dashed line).

Figure 7 shows twenty seconds of the large amplitude portion of the response of the SDOF system subjected to the base acceleration shown in Figure 6. The dotted line shows the uncontrolled response, the thick solid line shows the response of the system that uses time delayed PPF control with $\tau = 0.25$ and $\gamma_p = 0.5$, and the dashed line shows the response of the system that uses NPF control with no time delay and the same value of the control gain, $\gamma_p = 0.5$. Comparing the dotted line with the solid line in the figure, we observe that time delayed PPF control reduces the response amplitude of the system dramatically, while NPF control seems to have a much smaller effect. Also, the figure shows that the peak response of the time delayed system is reduced by a factor of two when compared with NPF control, again indicating that time delayed control is very much more effective than NPF control. Figure 8 shows a comparison of our time delayed control methodology ($\tau = 0.25$, $\gamma_p = 0.5$) and standard NPF control when using a much larger gain of $\gamma_p = 3$. We observe that despite the much larger control effort used in NPF control, the response amplitudes using time delayed PPF control are substantially smaller over most of the duration of the strong ground shaking.

To get a better feel for the improvement obtained when using time delayed control, in Figure 9 we show the *i*ntegral of the *s*quare of the *r*esponse (ISR) (over the entire 40 s duration of the base excitation) for the uncontrolled system, and the system with time delayed PPF control using $\gamma_p = 0.5$. Our time delayed PPF control reduces the ISR of the uncontrolled system (at the end of 40 s) by a factor of about 7! To explore the efficacy of this control, we compare it with two cases of NPF control using no time delay: one where the gain is the same as that used for the PPF control; the other, where the gain is increased to $\gamma_p = 3$. While NPF control with $\gamma_p = 0.5$

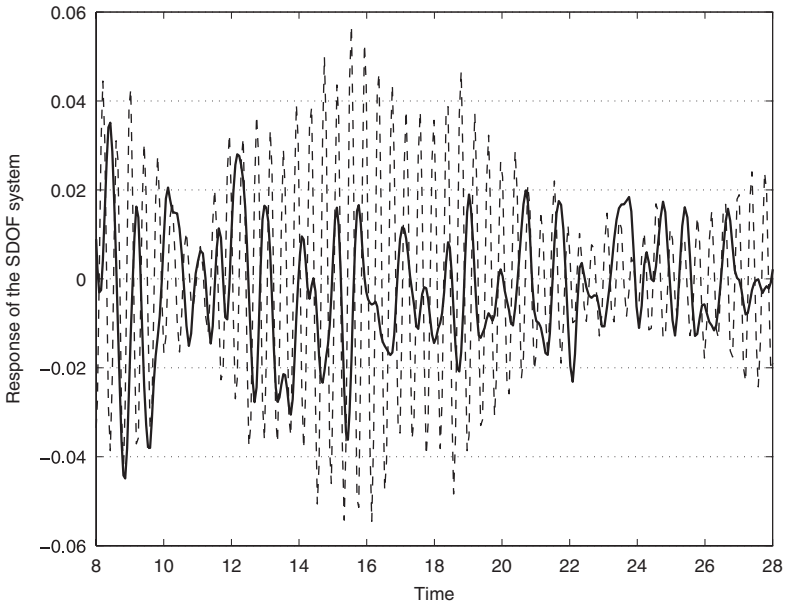

Figure 8. Comparison of the large amplitude response of the SDOF system when using PPF control with $\tau = 0.25$ and $\gamma_p = 0.5$ (solid line) and when using NPF control with no time delay and with $\gamma_p = 3$ (dashed line).

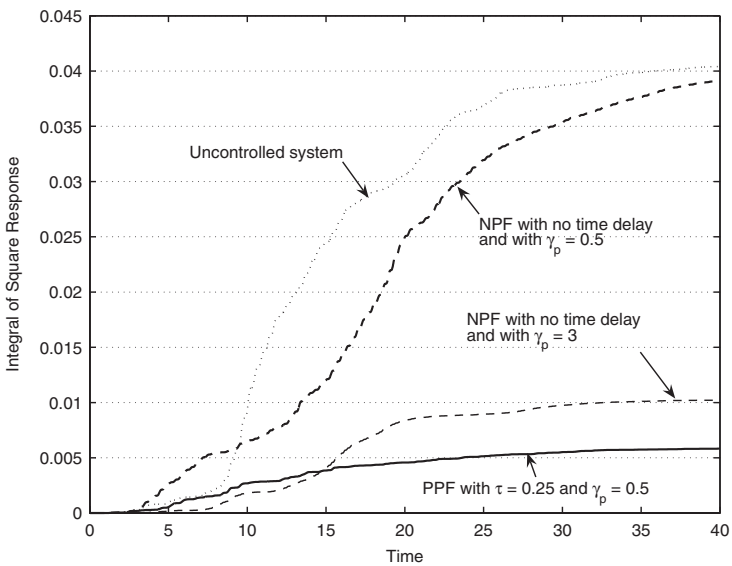

Figure 9. Comparison of the integral of the square of the response (ISR) of the SDOF system: using no control (dotted line); using PPF control with $\tau = 0.25$ and $\gamma_p = 0.5$ (thick solid line); using NPF control with no time delay with $\gamma_p = 0.5$ (thick dashed line); and using NPF control with no time delay with $\gamma_p = 3$ (thin dashed line).

appears to have little effect on the ISR of the controlled system at the end of 40 s, we see that the time delayed PPF control causes a dramatic drop in the ISR, which is lower than even the ISR for NPF control with $\gamma_p = 3$ by a factor of about 1.6. Thus, the chosen time delayed, proportional feedback control design appears to improve control performance significantly by substantially reducing the response of the system; and it also appears to be superior in performance when compared with the standard proportional feedback methodology. However, a fair comparison must also take into account the control effort required when using time delayed control as opposed to that required when using standard NPF control. And so this is what we turn to next.

Figure 10 shows a comparison of the control force required during the large amplitude response of the SDOF system. The solid line shows the control force required for PPF control with $\tau = 0.25$ and $\gamma_p = 0.5$ and the dashed line shows the control force required for NPF control with no time delay and the same gain, $\gamma_p = 0.5$. The peak value of the control force required for time delayed PPF is seen to be about *half* that required for NPF with no time delay. Figure 11 shows a similar comparison between our time delayed PPF control and NPF control with no time delay, but with a larger value of the gain $\gamma_p = 3$. The ratio of the peak force required using NPF (with $\gamma_p = 3$) to that required using our time delayed control is about 8, showing that a dramatic increase in control effort is required when the NPF control gain is increased from 0.5 to 3. And yet, as seen from Figures 8 and 9, NPF control with $\gamma_p = 3$ does not perform as well as time delayed PPF control with $\tau = 0.25$ and $\gamma_p = 0.5$.

This is further illustrated in Figure 12, which shows the *i*ntegral of the *s*quare of the *c*ontrol *f*orce (ISCF) required in the above-mentioned three cases over the entire duration of the base

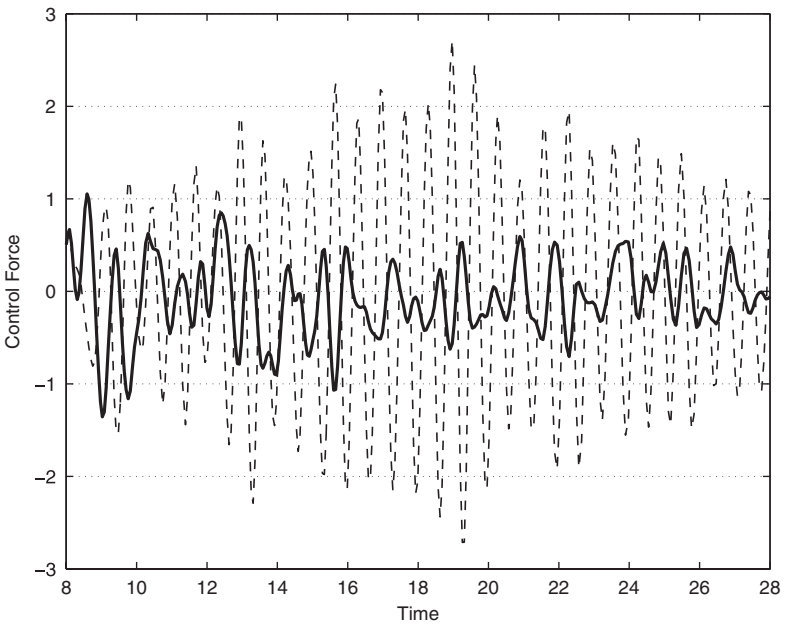

Figure 10. Comparison of the control force required for PPF control using $\tau = 0.25$ and $\gamma_p = 0.5$ (solid line) with that required for NPF control using no time delay and $\gamma_p = 0.5$ (dashed line).

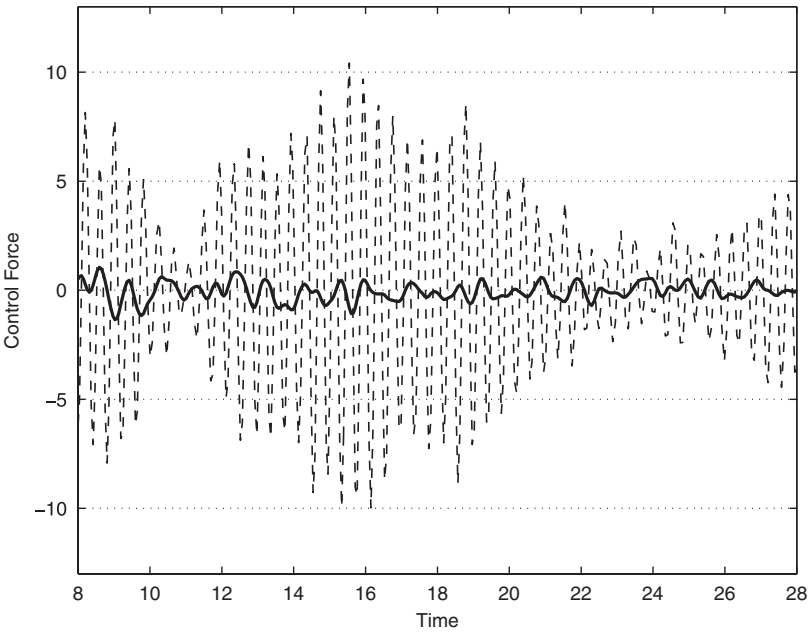

Figure 11. Comparison of the control force required for PPF control using $\tau = 0.25$ and $\gamma_p = 0.5$ (thick solid line) with that required for NPF control using no time delay and $\gamma_p = 3$ (thin dashed line).

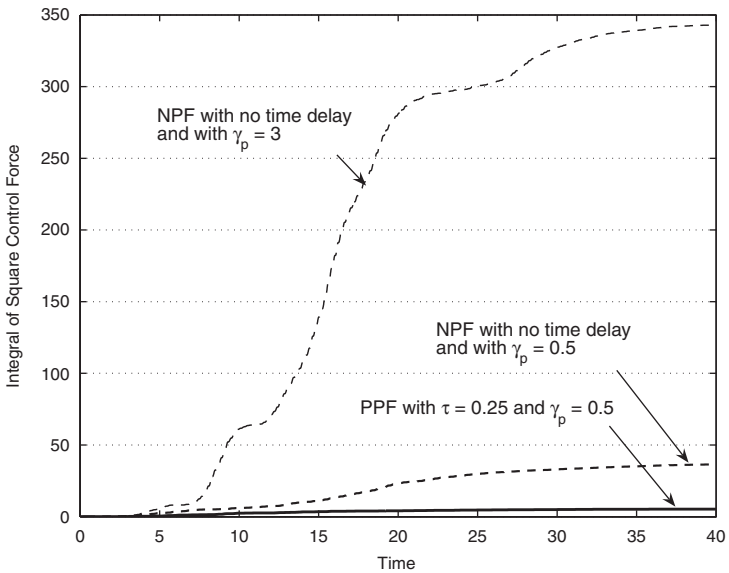

Figure 12. Comparison of the integral of the square of the control force (ISCF) of the SDOF system for: PPF control using $\tau = 0.25$ and $\gamma_p = 0.5$ (solid line); NPF control using no time delay and $\gamma_p = 0.5$ (thick dashed line); and NPF control using no time delay and $\gamma_p = 3$ (thin dashed line).

acceleration. As seen, the ratio at the end of 40 s of the ISCF when using NPF control with $\gamma_p = 0.5$ to that using time delayed PPF control, is about 6.65, indicating that more than a six-fold *smaller* control effort is required over the duration of the ground shaking when using the time delayed control strategy. Yet, the ISR at the end of 40 s for NPF control is more than 6 times that for the time delayed PPF control (see Figure 9), showing that the performance of the time delayed PPF control is about six-fold *superior*! When using NPF with $\gamma_p = 3$ the ratio of the control effort rises to about 68. Thus 68 times more control effort is required using NPF control with $\gamma_p = 3$ than with time delayed PPF control! And yet, the response amplitude reduction (see Figures 8 and 9) shown by time delayed PPF control is greater than that obtained using NPF control with $\gamma_p = 3$.

Standard negative proportional feedback (NPF) control is stable for all values of the control gain. As seen from Figure 5, the maximum gain for stability with time delayed PPF control when using $\tau = 0.25$ is unity. Thus, the response amplitude can, in principle, be continually reduced by continually increasing the gain for NPF control, something that cannot be done with the time delayed control design proposed herein since it becomes unstable beyond a gain of unity. However, the cost in the control effort when using NPF control becomes prohibitive when compared with the cost incurred when using time delayed control. This makes time delayed control an especially attractive alternative for structural applications. We have thus illustrated in this section that time delayed positive proportional feedback control designs can require far less control effort when compared with standard negative proportional feedback control and yet dramatically reduce the amplitude of the response of the system.

6. CONCLUSIONS

In this paper we explore the use of positive feedback proportional control using large, *intentional* time delays. From a practical standpoint, such time delays are easy and simple to implement in feedback control systems [19]. The proposed study indicates that time delays can be beneficially used in the control of structural systems. New results related to the stability and performance of time delayed, positive feedback proportional control are presented. We consider both system and non-system poles in our analysis, and our analytical results are validated computationally. We illustrate the performance of our control methodology by considering a structure modelled as a single-degree-of-freedom system subjected to an earthquake-like base acceleration. We show that time delayed, positive feedback proportional control, with a proper choice of control design parameters, while being amply stable, can be superior in controlling structural response when compared with standard (negative feedback) proportional control. Also, it is shown that time delayed positive feedback proportional control can require far less control effort than standard proportional control might require in order to achieve the same level of response reduction. That the proposed positive feedback control design is even feasible is not entirely intuitive; the fact that it can be extremely efficacious, even when compared with standard proportional negative feedback control, is even less so. The paper thus points to new and novel ways of controlling structural systems subjected to strong earthquake ground shaking. Studies on multi-degree-of-freedom systems are underway and will be reported shortly.

REFERENCES

1. Satche M. Stability of linear oscillating systems with constant time lag. *Journal of Applied Mechanics* 1949; **16**:419–420.
2. Choksy NH. Time lag systems. *Progress in Control Engineering* 1962; **1**:17–38.
3. Abdel-Rohman M. Structural control considering time delay effect. *Transactions of the Canadian Society for Mechanical Engineering* 1985; **9**:224–227.
4. Abdel-Rohman M. Time delays effects on actively damped structures. *Journal of Engineering and Mechanics* (ASCE) 1987; **113**:1709–1719.
5. Sain PM, Spencer BF, Sain MK, Suhardjo J. Structural control design in the presence of time delays. *Proceedings of the 9th Engineering Mechanics Conference*, ASCE, College Station, 24–27 May 1992.
6. Agarwal AK, Fujino Y, Bhartia B. Instability due to time delay and its compensation in active control of structures. *Earthquake Engineering and Structural Dynamics* 1993; **22**:211–224.
7. Agarwal AK, Yang JN. Effect of fixed time delay on stability and performance of actively controlled civil engineering structures. *Earthquake Engineering and Structural Dynamics* 1997; **26**:1169–1185.
8. Agarwal AK, Yang JN. Compensation for time delay for control of civil engineering structures. *Earthquake Engineering and Structural Dynamics* 2000; **29**:37–62.
9. Marshall JE. Extensions of O.J. Smith's method to digital, other systems. *International Journal of Control* 1974; **19**:933–939.
10. Udwadia FE, Kumar R. Time delayed control of classically damped structural systems. *International Journal of Control* 1994; **60**:687–713.
11. Kobori T, Koshika N, Yamada Y, Ikeda Y. Seismic-response-controlled structure with active mass driver system, Part 1: design. *Earthquake Engineering and Structural Dynamics* 1991; **20**:133–149.
12. Koike Y, Murata T, Tanida K, Mutaguchi M, Kobori T, Ishii K, Takenaka Y, Arita T. Development of v-shaped hybrid mass damper and its application to high-rise buildings. *Proceedings of the 1st World Conference on Structural Control*, vol. FA2-3–FA2-12, 1994.
13. Udwadia FE. Noncollocated point control of nondispersive continuous systems using time delays. *Applied Mathematics and Computation* 1991; **42**(1):23–63.
14. Udwadia FE. Noncollocated control of continuous systems with tip-inertias. *Applied Mathematics and Computation* 1992; **47**:47–75.
15. Udwadia FE, Kumar R. Time delayed control of classically damped structures. *Proceedings of the 11th World Conference on Earthquake Engineering*, Acapulco, Mexico, 23–28 June 1994.
16. von Bremen H, Udwadia FE. Can time delays be useful in the control of structural systems? *Proceedings of the 42nd AIAA/ASME/ASCE/AHS Structures, Dynamics and Materials Conference*, Atlanta, 3–6 April 2000.
17. von Bremen H, Udwadia FE. Effect of time delay on the control of a torsional bar. *Proceedings of the 43rd AIAA/ASME/ASCE/AHS Structures, Dynamics and Materials Conference*, Seattle, 16–19 April 2001.
18. Udwadia FE, von Bremen H, Kumar R, Hosseini M. Time delayed control of structures. *Earthquake Engineering and Structural Dynamics* 2002; **32**:495–535.
19. Udwadia FE, von Bremen H, Phohomsiri P. Time delayed control design for active control of structures: principles and application. *Structural Control and Health Monitoring* 2006; DOI: 10.1002/stc.82, in press.
20. Phohomsiri P, Udwadia FE, von Bremen H. Time delayed positive velocity feedback design for active control of structures, to appear in the *Journal of Engineering Mechanics*.
21. Olgac N, Holm-Hansen BT. A novel active vibration absorption technique: delayed resonator. *Journal of Sound and Vibration* 1994; **176**:93–104.
22. Olgac N, Elmali H. Analysis and design of delayed resonator in discrete domain. *Journal of Vibration and Control* 2000; **6**:273–289.

